



## Myeloperoxidase enhances the migration and invasion of human choriocarcinoma JEG-3 cells

Z.N. Mihalic<sup>a</sup>, T. Kloimböck<sup>a</sup>, N. Cosic-Mujkanovic<sup>a</sup>, P. Valadez-Cosmes<sup>a</sup>, K. Maitz<sup>a</sup>, O. Kindler<sup>a</sup>, C. Wadsack<sup>b,c</sup>, A. Heinemann<sup>a,c</sup>, G. Marsche<sup>a,c</sup>, M. Gauster<sup>d</sup>, J. Pollheimer<sup>e</sup>, J. Kargl<sup>a,c,\*</sup>

<sup>a</sup> Otto Loewi Research Center, Division of Pharmacology, Medical University of Graz, Austria

<sup>b</sup> Department of Obstetrics and Gynecology, Medical University of Graz, Austria

<sup>c</sup> BioTechMed-Graz, 8010, Graz, Austria

<sup>d</sup> Division of Cell Biology, Histology and Embryology, Medical University of Graz, Austria

<sup>e</sup> Department of Obstetrics and Gynecology, Reproductive Biology Unit, Maternal-Fetal Immunology Group, Medical University of Vienna, Austria

### ARTICLE INFO

#### Keywords:

Neutrophils  
Myeloperoxidase  
Trophoblasts  
Decidua basalis  
Cell migration

### ABSTRACT

Myeloperoxidase (MPO) is one of the most abundant proteins in neutrophil granules. It catalyzes the production of reactive oxygen species, which are important in inflammation and immune defense. MPO also binds to several proteins, lipids, and DNA to alter their function. MPO is present at the feto-maternal interface during pregnancy, where neutrophils are abundant. In this study, we determined the effect of MPO on JEG-3 human choriocarcinoma cells as a model of extravillous trophoblasts (EVTs) during early pregnancy. We found that MPO was internalized by JEG-3 cells and localized to the cytoplasm and nuclei. MPO internalization and activity enhanced JEG-3 cell migration and invasion, whereas this effect was impaired by pre-treating cells with heparin, to block cellular uptake, and MPO-activity inhibitor 4-ABAH. This study identifies a novel mechanism for the effect of MPO on EVT function during normal pregnancy and suggests a potential role of MPO in abnormal pregnancies.

### 1. Introduction

Pregnancy is an immunological challenge, in which the mother and fetus must coexist. During early pregnancy, placenta-derived extravillous trophoblasts (EVTs) invade the decidua, engraft and remodel uterine spiral arteries. They gradually replace maternal endothelial cells to enable an adequate blood flow into the placenta [1]. Therefore, it is important that this process is highly regulated as defective EVT invasion results in abnormal placentation. Maternal immune cells represent 30%–40% of all decidual cells [2]. Maternal leukocytes, particularly uterine natural killer cells, regulate EVT invasion and are important for normal development during pregnancy [3]. However, other maternal immune cells, such as neutrophils, are also required for developing a healthy feto-maternal interface, which are highly present in the decidua basalis (DB) [4]. Neutrophils are part of the innate immune system and one of the first cell types that respond to acute inflammation. Neutrophil

infiltration during pregnancy occurs at the DB [5,6]. The depletion of neutrophils in mouse models results in abnormal placentation [7]; however, the role and interactions of neutrophils with EVT function remain unclear.

Myeloperoxidase (MPO) is a heme-bound enzyme primarily expressed in the azurophilic granules of neutrophils but is also present in monocytes and macrophages [8]. It represents 5% of the whole neutrophil cell weight, making it one of the most abundant proteins in neutrophils [9]. Upon neutrophil activation, MPO is transported into phagosomes or released into the extracellular space [10]. It catalyzes the production of reactive oxygen species (ROS), such as hypochlorous acid (HOCl), in an oxidative reaction of hydrogen peroxide with (pseudo) halides (chloride, bromide, iodide and thiocyanate), which are important for pathogen killing during infections [11]. MPO is highly positively charged because of its high arginine and lysine content; therefore, it also binds to various proteins, DNA, and lipids [12]. Independent of its

*Abbreviations:* DB, Decidua basalis; ECIS, Electric cell-substrate impedance sensing; EMEM, Earle's Minimum Essential Medium; EVT, Extravillous trophoblasts; FBS, Fetal bovine serum; ROS, Reactive oxygen species.

\* Corresponding author. Otto Loewi Research Center, Division of Pharmacology, Medical University of Graz, Austria.

E-mail address: [julia.kargl@medunigraz.at](mailto:julia.kargl@medunigraz.at) (J. Kargl).

<https://doi.org/10.1016/j.redox.2023.102885>

Received 13 April 2023; Received in revised form 8 September 2023; Accepted 11 September 2023

Available online 19 September 2023

2213-2317/© 2023 The Authors. Published by Elsevier B.V. This is an open access article under the CC BY license (<http://creativecommons.org/licenses/by/4.0/>).

catalytic activity, MPO can bind to CD11b/CD18 integrins on the surface of neutrophils, resulting in neutrophil activation, delaying apoptosis and increasing their lifespan [13,14]. Further, MPO binds to proteins in the extracellular matrix and modifies them through HOCl [15]. Additionally, MPO can bind to DNA [16], and has roles in lipid modification, apoptosis regulation, neutrophil extracellular trap (NET) formation, and macrophage interactions [8,17]. MPO and HOCl play fundamental roles in releasing neutrophil elastase during NET formation [18]. Furthermore, MPO affects the angiogenesis of endothelial cells [19].

In the placenta, the presence of neutrophils and MPO in the DB has been confirmed [4–7,20,21]. Furthermore, higher MPO levels on the surface of blood neutrophils have been observed during pregnancy [22]; however, its abundance and role during first trimester implantation and placentation remains unclear. Therefore, we examined the role and uptake of MPO using the JEG-3 EVT model cell line. We hypothesized that MPO affects JEG-3 function in vitro and that its effects depend on MPO internalization. Our results indicate that the JEG-3 uptake of MPO stimulated their migration and invasion, which may represent a drug target for pregnancy complications associated with shallow trophoblast invasion.

## 2. Material and methods

### 2.1. Human tissue samples

Decidual tissues from the first trimester (6–10 weeks of gestation) were obtained from women who underwent elective pregnancy termination for nonmedical purposes. The pregnancy terminations were conducted through surgical aspiration. The utilization of patient material was approved by the Ethics Committee of the Medical University of Vienna and the Medical University of Graz (both Austria).

### 2.2. Cell culture

Human placental-epithelial choriocarcinoma cells (JEG-3 HTB-36TM ATCC®) were cultured in Earle's Minimum Essential Medium (EMEM+/+) (Gibco™) containing 2-mM L-glutamine supplemented with 1% nonessential amino acids (Gibco™), 1 mM sodium-pyruvate (Gibco™), 10% fetal bovine serum (FBS) (Gibco™) and 1% penicillin/streptomycin (P/S) (Gibco™) at 37 °C and 5% CO<sub>2</sub>. Before treatment, the cells were starved for 4 h in starvation medium (EMEM–/–) (EMEM without FBS, P/S, nonessential amino acids, and sodium-pyruvate) and treated with the indicated concentrations of MPO (Elastin products company), in combination with 150 µg/ml heparin (Gilvasan, 1000 IE/ml) or 400 µM 4-aminobenzoic acid hydrazide (4-ABAH) (Sigma-Aldrich) where applicable. As a control (VEH), starvation media was used.

### 2.3. Immunofluorescence staining

Paraffin-embedded placenta sections prepared from first trimester elective pregnancy terminations were heated at 60 °C, immersed in xylene, rehydrated in descending alcohol concentrations (100%, 96%, 80%, 70%, 50%), washed in phosphate-buffered saline (PBS) without Ca<sup>2+</sup> and Mg<sup>2+</sup> (PBS–/–), and boiled in antigen retrieval buffer (2.94-g/L tri-sodium dihydrate, MW 294 g, pH = 6) for 15 min. Cold antigen retrieval buffer was added and cooled to 4 °C for 1 h. The slides were washed in PBS–/–, incubated for 30 min in 0.3% H<sub>2</sub>O<sub>2</sub> (in PBS–/–), and subsequently washed in PBS–/–. The slides were incubated in blocking solution [0.3% TRTX, 5% goat serum, 4% BSA (Sigma-Aldrich) in PBS–/–] at room temperature for 1.5 h and subsequently incubated with primary rabbit anti-MPO antibody (Cell Signaling, clone: E1E71, 1:500) and primary mouse anti-HLA-G antibody (BD, clone: 4H84, 1:2500) in a humidified box at 4 °C overnight. The slides were washed again and incubated in goat anti-rabbit AlexaFluor488 (Invitrogen, 1:500) and goat anti-mouse AF647 (Invitrogen, 1:500) secondary

antibody for 3 h in the dark. The slides were then washed in PBS–/– and background was reduced using Vector True View Kit mix for 3 min. The slides were washed in PBS–/– and the nuclei were stained with Vecta Shield Mounting Medium containing DAPI (Szabo Scandic).

### 2.4. MPO enzyme-linked immunosorbent assay

Tissue was collected from elective first trimester abortions and separated into DB and decidua parietalis (DP), as previously described [4]. Tissue pieces were incubated at 37 °C for 24 h in 0.5 ml F12/DMEM without phenol red media but supplemented with 1% P/S, and supernatant was collected. Enzyme-linked immunosorbent assay was performed and analyzed according to the manufacturers' protocol (Human Myeloperoxidase DuoSet ELISA, R&D Systems, #DY3174).

### 2.5. MPO RNA expression

Basal plate RNA expression data [23] were acquired from the dataset GSE22490 of the NCBI Gene Expression Omnibus database (GEO) (<http://www.ncbi.nlm.nih.gov/geo/>) via the R package GEOQuery (n = 10). MPO expression was plotted with the help of R package ggplot. (R version 4.2.2) [24,25].

### 2.6. Immunocytochemistry

JEG-3 cells were seeded into 6-well plates on coverslips in growth medium, incubated for 24 h, and subsequently starved overnight. Afterwards, the cells were treated for 4h in starvation medium with 10 µg/ml of MPO (Elastin Products Company) or 5 µg/ml MPO in combination with heparin and 4-ABAH. Heparin and 4-ABAH were added directly prior to MPO treatment. Afterwards, the coverslips were washed with PBS–/–, the cells were fixed with 100% ice-cold methanol for 20 min at –20 °C, and subsequently washed with PBS–/–. Blocking was performed in PBS–/– supplemented with 5% goat serum (Sigma-Aldrich) and 5% BSA (Sigma-Aldrich) for 1 h at RT. A primary rabbit anti-MPO antibody (Cell Signaling, 1:500) in 1:10 blocking solution + 0.1% Triton X-100 was added and incubated overnight at 4 °C. After washing with PBS–/–, the coverslips were incubated with secondary antibody (goat anti-rabbit AlexaFluor488 (Invitrogen, 1:500) for 1 h at RT followed by another washing step. The coverslips were mounted along with DAPI (Vecta Shield Mounting Medium) on glass slides. The cells were observed using an Olympus IX70 fluorescence microscope equipped with a Hamamatsu ORCA-ER digital camera (Hamamatsu Photonics K. K., Japan). CellSense 1.17 Dimension software was used for processing the images.

### 2.7. Bromodeoxyuridine proliferation assay

Following treatment with MPO [VEH, 0.5, 2, 5 µg/ml] for 24, 48, and 72 h, 10 µM bromodeoxyuridine (BrdU) solution was added 4 h before the end of the experiment [fluorescein isothiocyanate (FITC) BrdU Flow Kit (BD #559619)] according to the manufacturers' protocol. Briefly, the cells were washed in PBS–/– and stained with Fixable Viability Dye eFluor™ 450 (Thermo Scientific) for 20 min. Afterwards, the cells were washed in PBS–/– and permeabilized using Cytofix/Cytoperm buffer (BD) for 20 min. Following fixation, the cells were washed in 1X BD Perm/Wash Buffer and treated with 30-µg/ml DNase I for 1 h at 37 °C. The cells were washed and stained with FITC-conjugated BrdU Antibody (1:50) prepared in Perm/Wash buffer (BD) for 20 min. Upon stimulation, the cells were again washed, and proliferation was measured by flow cytometry.

### 2.8. Annexin V apoptosis assay

After treatment with 5 µg/ml MPO for 6, 15, 18, and 24 h, the cells were stained in 1x Annexin V Binding Buffer and incubated with FITC-

anti human Annexin V antibody (1:50) and PI (1:50) for 15 min, according to the manufacturers' instructions, as previously described [26].

## 2.9. Scratch assay

Cells ( $6 \times 10^5$ /well) were seeded into 6-well plates, grown for 24 h, and subsequently starved in starvation medium for 5 h. The starved cells were washed with PBS $^{-/-}$  and subsequently scratched using a SPLScarTM Scratcher suitable for 6-well plates (SPL Life Science). The cells were washed and treated with 0  $\mu$ g/ml, 2.5  $\mu$ g/ml or 5  $\mu$ g/ml MPO. Light microscopy images were captured at 100x magnification (Nikon) directly after wounding and after 24 h. To calculate the amount of wound closure, the cell-free area was determined using ImageJ software. Wound closure after 24 h is presented as the fold-change percentage of the initial wound area.

## 2.10. Electric cell-substrate impedance-sensing migration assay

Electric cell-substrate impedance sensing (ECIS) was performed in a 96W1E + plate (96-well array from Applied BioPhysics). The wells were activated using 10-mM L-cysteine (Sigma-Aldrich) for 10 min at RT. Afterwards, the wells were washed twice with water and once with growth medium. Cells ( $4.8 \times 10^5$ /well) were seeded and incubated for 48 h. Confluent cells were starved overnight. Resistance was measured at 4000 Hz (ECIS $^{\text{®}}$  Z $\theta$ ) and wounding was performed in each well at 3000  $\mu$ A and 48 000 Hz for 30 s. Afterwards, the cells were treated with 0  $\mu$ g/ml, 1  $\mu$ g/ml, 2.5  $\mu$ g/ml, 5  $\mu$ g/ml, and 10  $\mu$ g/ml MPO, and 5  $\mu$ g/ml MPO in combination with heparin and 4-ABAH. Resistance was measured for 24 h in 60 s intervals and expressed as fold-change relative to the baseline resistance before wounding. Post-wounding values were subtracted for normalization and represented as the mean of at least eight replicates per condition in each individual experiment.

## 2.11. Invasion

Cells ( $1.5 \times 10^5$ /well) were seeded into six-well plates in 2 ml EMEM $^{+/+}$  and incubated for 24 h. The cells were detached with Accutase (Sigma-Aldrich) and washed in PBS $^{-/-}$ , starved for 4 h, and treated with vehicle or 5  $\mu$ g/ml MPO. A 24-well invasion chamber (#354480 Corning) was used. The chamber was activated by the addition of warm (37  $^{\circ}$ C) EMEM $^{-/-}$  to the interior of the inserts (0.5 ml) and bottom of the wells (0.5 ml) for 2 h. Upon activation, the medium was removed, and 750  $\mu$ l EMEM $^{+/+}$  was added to the bottom well. The treated cell suspension was added to the insert and incubated for 24 h at 37  $^{\circ}$ C, and 5% CO $_2$ . Afterwards, non-invaded cells were removed from the upper part of the membrane by wiping with cotton swab over the membrane of the chamber. The invaded cells were fixed and stained with Diff-Quick solution. A scalpel was used to remove the membrane from the insert and placed on a microscopy slide. Five photos of each membrane were captured at 100  $\times$  magnification using Olympus B $\times$ 53 with an Olympus UC90 camera. CellSense Standard software was used. ImageJ software (R Foundation) cell counter function was used to count the invaded cells.

## 2.12. Nuclear and cytoplasmic fractionation of JEG-3 cells

Cells ( $5 \times 10^5$ ) were seeded into 10 cm dishes and incubated until confluent. The cells were starved for 4 h and subsequently incubated with 10  $\mu$ g/ml MPO for 2 h. Afterwards, the cells were washed in PBS $^{-/-}$ , 1 ml of ice-cold PBS $^{-/-}$  was added, and the cells were scraped. The cells were pelleted for 5 min at 13,000 rpm (4  $^{\circ}$ C) and the supernatants were aspirated. Next, 500  $\mu$ l Buffer A [10 mM HEPES, 10 mM KCl, 0.1 mM EDTA, protease/phosphatase inhibitor (100  $\times$ ), (Cell Signaling) in PBS $^{-/-}$  was added. Cells were homogenized for 15 s at medium power on ice. Then, 25  $\mu$ l NP-40 was added and thoroughly mixed by vortex mixing. Lysates were centrifuged for 5 min at 5000 rpm at 4  $^{\circ}$ C.

Supernatants were separated (cytoplasmic fraction) from the remainder and stored on ice. For nuclear fractions, the pellets were mixed with 50  $\mu$ l ice-cold buffer C (20-mM HEPES pH 7.9, 25% glycerol, 0.4-M NaCl, 1-mM EDTA in PBS $^{-/-}$ ). The pellet was gently dislodged and afterwards vigorously rocked on ice for 30 min. Lysates were centrifuged for 10 min at 14,000 rpm at 4  $^{\circ}$ C. The supernatant (nuclear fraction) was collected and both fractions were used for Western blot analysis.

## 2.13. Western blot analysis

Total protein was isolated from frozen cells in IP buffer (0.1% Triton X-100, 150-mM NaCl, 25-mM KCl, 10-mM Tris HCl, pH 7.4; 1-mM CaCl $_2$  in H $_2$ O) supplemented with 1:100 protease/phosphatase inhibitor cocktail (Cell Signaling). The protein content was measured using a Pierce BCA assay kit (Thermo Scientific). Protein concentration for each sample was adjusted to 1 mg/ml, using IP buffer. The samples were mixed with 4  $\times$  NuPage sample buffer (90  $\mu$ l 4  $\times$  LDS sample buffer + 10  $\mu$ l reducing reagent) and boiled for 10 min at 95  $^{\circ}$ C. Next, 20  $\mu$ g of protein from each homogenate was applied to the NuPage, Bis-Tris gel (Invitrogen) and electrophoresed for 45 min at 200 V. The proteins were transferred to a membrane using an iBlot transfer device and blocked in TBST (1  $\times$  TBS + 0.1% Tween) supplemented with 5% milk for 1 h. The membrane was incubated with the primary antibody overnight at 4  $^{\circ}$ C. Anti-MPO (rabbit antihuman MPO, clone: E1E71, 1:500 dilution, Cell Signaling), anti-GAPDH (rabbit anti-human GAPDH, clone: 14C10, 1:500 dilution, Cell Signaling), anti-Lamin A/C (mouse anti-human Lamin A/C, clone: 4C11, 1:1000 dilution, Cell Signaling), and anti-AKT (rabbit anti-human Akt, clone: 11E7, 1:1000 dilution, Cell Signaling) monoclonal antibodies were used. The membranes were washed for 30 min and subsequently incubated with secondary antibody HRP-Goat anti-rabbit IgG (polyclonal, 1:5000 dilutions, Jackson ImmunoResearch) for 2 h at RT. The membranes were washed and developed using ECL solution (BioRad).

## 2.14. Flow cytometry

Cells ( $3 \times 10^5$ /well) were seeded into 6-well plates and incubated for 24 h. The cells were then starved overnight and treated with 2.5- and 5- $\mu$ g/ml MPO or MPO in combination with heparin and 4-ABAH for 4 h. The cells were fixed and permeabilized for 40 min using a BD transcription factor fixation/permeabilization kit to allow the antibodies to bind to nuclear protein. Subsequently, the cells were preincubated with Fc receptor blocking solution followed by anti-human MPO-FITC-conjugated antibody (BD) for 30 min at 4  $^{\circ}$ C, washed twice in TF washing buffer (BD), and once in PBS without PBS $^{-/-}$  supplemented with 2% FBS. Samples were measured using a Canto II flow cytometer with FACSDiva software (BD). Analysis and compensation were performed using FlowJo software (TreeStar).

## 2.15. Myeloperoxidase activity

MPO activity was measured as previously described [27]. Briefly, cells ( $3.5 \times 10^5$ /well) were seeded into 6-well plates in 2 ml EMEM $^{+/+}$  and incubated for 24 h. The cells were then starved for 4 h and treated for 4 h with 5  $\mu$ g/ml MPO or MPO in combination with heparin and 4-ABAH + 25  $\mu$ M H $_2$ O $_2$ . The cells were detached with Accutase (Sigma-Aldrich) and washed in PBS $^{-/-}$ . The cells were resuspended in 500  $\mu$ l inhibitor cocktail (1:100 dilution in PBS $^{-/-}$ ), sonicated for 15 s on ice and centrifuged for 10 min at 18,000 rpm (4  $^{\circ}$ C). In a 96-well plate, 100  $\mu$ l of 3,3',5,5'-tetramethylbenzidine solution + H $_2$ O $_2$  (BioLegend; ELISA detection reagent A + B; 1:1) were prepared and 5  $\mu$ l of sample supernatant was added. The reaction was incubated for 30 min in the dark and stopped with 50  $\mu$ l 2-N sulfuric acid. The absorbance was measured at 450 nm. To confirm the inhibitory capacity of 4-ABAH, we measured MPO activity after 5 min in EMEM $^{-/-}$  with 5  $\mu$ g/ml MPO with and without 4-ABAH and 25  $\mu$ M of H $_2$ O $_2$ .

## 2.16. Statistical analysis

GraphPad Prism 9.1 (GraphPad Software) and R software were used to perform statistical analyses. Statistically significant differences between two groups were determined using unpaired students t-test. To compare more than two groups, one-way ANOVA followed by the Turkey's post hoc test was used. A P-value <0.05 was considered statistically significant.

## 3. Results

### 3.1. Neutrophils are located near extravillous trophoblasts in the first-trimester DB

There is little information regarding the localization and interaction of neutrophils and EVT's in the DB during the first trimester of pregnancy. Consequently, we determined the localization of MPO, used as a marker for neutrophils, and EVT's (detected by HLA-G) in first trimester DB. We observed MPO-positive neutrophils (green) in close proximity to HLA-G positive EVT's (magenta) via fluorescence immunohistochemistry (Fig. 1a). Consistent with our data, it has been previously shown that MPO accumulates in human placenta and the DB during the third trimester of pregnancy [20]. To confirm MPO release from first-trimester decidua neutrophils, we used MPO ELISA to measure MPO levels in tissue explant supernatants from matched DB and DP samples from elective abortions (Fig. 1b). We confirmed higher levels of MPO in the DB compared to DP. Further, we investigated a

publicly-available bulk microarray dataset for the expression of MPO in the first-trimester basal plate [23]. We observed MPO expression in all samples (Fig. 1c). Each bar represents a separate sample.

### 3.2. Myeloperoxidase increases JEG-3 migration and invasion in vitro

The JEG-3 choriocarcinoma cell line serves as a model to study EVT cell behavior in the presence of MPO as primary trophoblasts lack sufficient proliferation in vitro [28]. To assess the effect of MPO on JEG-3 cells, we performed AnnexinV/PI staining to determine if MPO affects JEG-3 apoptosis. We measured live (AnnexinV-/PI-), early apoptotic (AnnexinV+/PI-), late apoptotic (AnnexinV+/PI+), and dead (AnnexinV-/PI+) cells at 6 h, 15 h, 18 h, and 24 h of treatment (Fig. 1d, Supplementary Fig. 1a). Furthermore, we exposed cells to various concentrations of MPO and measured the effect on cell proliferation after 24 h, 48 h, and 72 h of treatment. We did not observe any differences in proliferation of JEG-3 cells between exposure to vehicle and to increasing concentrations of MPO (0.5, 2, and 5 µg/ml) at any timepoint (Fig. 1e). Similar to the proliferation assay, we did not observe any effect of MPO on JEG-3 apoptosis compared with untreated cells. Apoptosis and proliferation data are presented as fold change in Fig. 1d and e and as % of all cells in the Supplementary Figs. 1 and 2). During normal/healthy early pregnancy, EVT's migrate and invade in large numbers toward the maternal spiral arteries to supply adequate blood flow to the fetus [29]. During pregnancy complications, such as pre-eclampsia and intrauterine growth restriction (IUGR), EVT's do not invade deeply enough, which affects spiral artery remodeling [30]. Because EVT

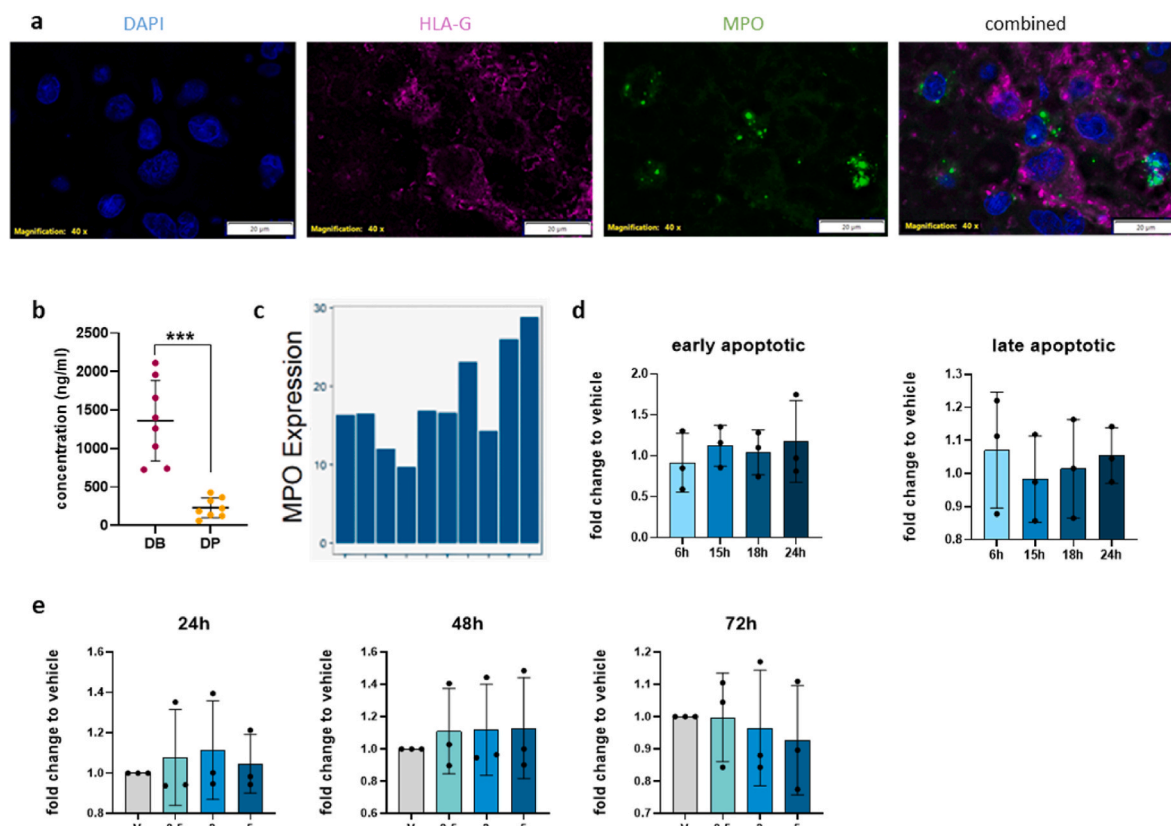


**Fig. 1.** MPO is present in decidua basalis

**a**) Representative immunofluorescence microscopy of first trimester decidua basalis. Slides were stained for HLA-G (magenta) and MPO (green). **b**) MPO concentration in DB and DP of first trimester pregnancy explant supernatants using ELISA (N = 8). Paired t-test was performed. Data are represented as the mean  $\pm$  SD, \*P < 0.05. **c**) MPO expression in basal plate of publicly available microarray data. Each bar represents a separate sample (N = 10). **d**) JEG-3 Annexin V/PI apoptosis assay. Early apoptotic and late apoptotic cells were measured by flow cytometry following treatment with 5 µg/ml MPO. Annexin V and PI were measured at 6 h, 15 h, 18 h, and 24 h following MPO treatment and compared with vehicle-treated cells (N = 3). **e**) Proliferation of JEG-3 cells after 24 h, 48 h, and 72 h treatment with vehicle or 0.5 µg/ml, 2 µg/ml, and 5 µg/ml MPO (N = 3). One-way analysis of variance (ANOVA) and Tukey's post hoc test were performed. Data are represented as the mean  $\pm$  SD, \*P < 0.05. (For interpretation of the references to colour in this figure legend, the reader is referred to the Web version of this article.)

migration is a key feature in normal placentation, we determined if MPO affects this process. First, we conducted a wound-healing assay using JEG-3 cells (Fig. 2a). JEG-3 cells treated with 2.5  $\mu\text{g}/\text{ml}$  MPO did not significantly increase wound closure after 24 h; however, there was a trending increase in migration of treated cells compared with the control. Upon treatment with 5  $\mu\text{g}/\text{ml}$  MPO, JEG-3 cells showed significantly enhanced levels of migration compared with the vehicle treated group (Fig. 2b, Supplementary Fig. 3a). To confirm this effect, we performed an ECIS migration assay at four different MPO concentrations (1–10  $\mu\text{g}/\text{ml}$ ) for up to 24 h (Fig. 2c, Supplementary Fig. 3b). At 14 h post-wounding, enhanced wound closure was observed in MPO-treated JEG-3 cells compared with the control cells (Fig. 2d). Due to the importance of EVT invasion in the development of pregnancy complications [31] and our finding of the effect of MPO on migration, we determined if MPO also influences the ability of EVTs to invade. Similar, to migration, we identified enhanced invasion of JEG-3 cells upon MPO treatment (Fig. 2e and f, Supplementary Fig. 3c).

### 3.3. Myeloperoxidase uptake by JEG-3 cells and nuclear localization

MPO binds to the surface of endothelial and epithelial cells through binding to glycosaminoglycans and is rapidly internalized by the exposed cells [32]. To determine if MPO is taken up by JEG-3 cells, we treated JEG-3 cells with increasing MPO concentrations, cells were washed thoroughly to remove remaining MPO in the media and then

MPO protein levels were measured by Western blot analysis. The total MPO protein amount increased in JEG-3 cells treated with higher concentrations (Fig. 3a). Immunofluorescence microscopy of vehicle and MPO-treated JEG-3 cells revealed that untreated cells did not contain MPO. Upon treatment, MPO was internalized and localized to the cytoplasm and nuclei (Fig. 3b). Furthermore, we observed that not all the cells bind or take up MPO, which was confirmed by flow cytometry (Fig. 3c and d). We stained for MPO following nuclear permeabilization and observed that upon treatment with 2.5  $\mu\text{g}/\text{ml}$  and 5  $\mu\text{g}/\text{ml}$  of MPO, approximately 4% and 9% of the cells, respectively, internalized MPO (Fig. 3c and d). To assess MPO intracellular localization following uptake, the cells were separated into cytoplasmic and nuclear fractions following 5  $\mu\text{g}/\text{ml}$  MPO treatment for 2 and 24 h. MPO was observed in both the cytoplasmic and nuclear fraction at each time point (Fig. 3e). To confirm the purity of these fractions, Lamin A/C was present only in the nuclear fraction and tAKT was more abundant in the cytoplasmic fraction (Fig. 3e). The MPO signal cannot be quantified and compared between the different fractions due to the different buffers and volumes used for isolation of the fractions. MPO activity assays revealed that MPO was active upon cell uptake and was measured in cell lysates after 4 h of treatment (Fig. 3f). Next, the activity of MPO was investigated in nuclear and cytoplasmic fractions, which were isolated upon MPO treatment of JEG-3 cells with 5  $\mu\text{g}/\text{ml}$  MPO. The results are represented as fold change toward untreated cells. In both fractions, MPO activity was measured, suggesting that MPO remains active even after

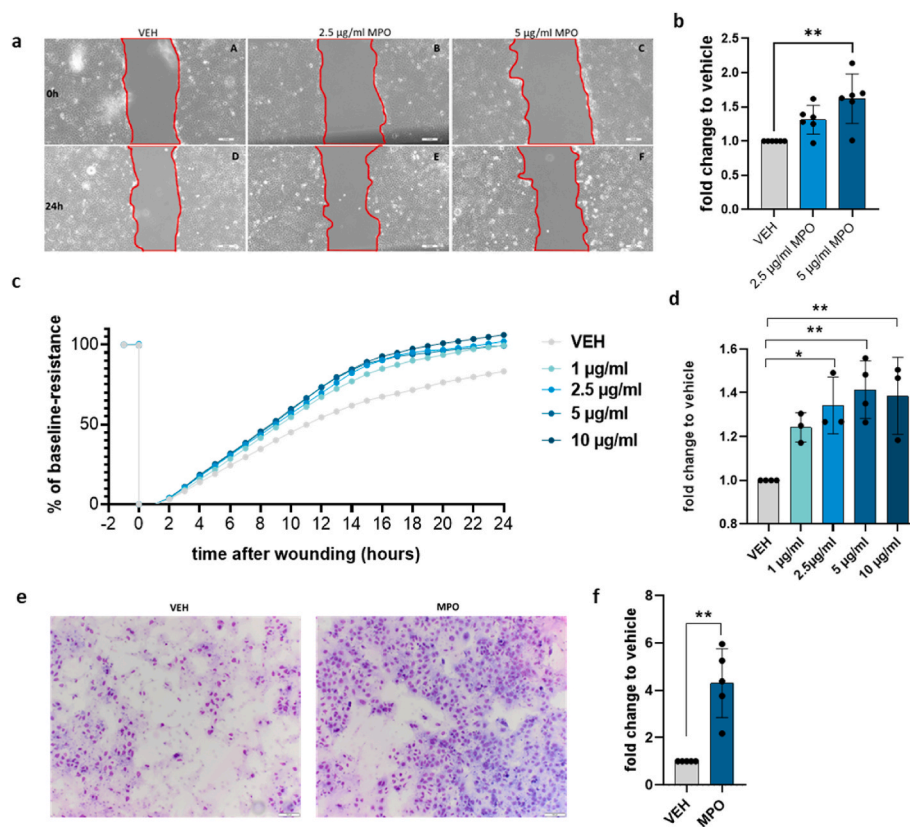


**Fig. 2.** MPO alters JEG-3 migration and invasion in vitro

**a)** Scratch migration assay of JEG-3 cells treated with vehicle, 2.5  $\mu\text{g}/\text{ml}$ , and 5  $\mu\text{g}/\text{ml}$  MPO. Microscopic images were taken immediately (A–C) and 24 h (D–F) after wounding. **b)** Scratch assay results are presented as % cell-free area at time 0 and after 24 h normalized to the vehicle-treated cells (N = 6). **c)** Wound closure capacity of JEG-3 cells measured by ECIS (N = 3–4) after treatment with 1  $\mu\text{g}/\text{ml}$ , 2.5  $\mu\text{g}/\text{ml}$ , 5  $\mu\text{g}/\text{ml}$ , and 10  $\mu\text{g}/\text{ml}$  MPO. The cell monolayer was wounded at 3000  $\mu\text{A}$  and 48000 Hz for 30 s (t = 0). Post-wounding resistance values were normalized to the wounding efficiency by subtracting the resistance value after wound induction from all values. Wound closure was monitored over 24 h and expressed as fold-change compared with baseline resistance before wounding (baseline resistance: 100 = monolayer, 0 = wounding). **d)** Results of ECIS measurements represented as mean (normalized to the % of wounding) fold-change relative to the vehicle after 14 h. **e)** Representative images of the invasion assay of vehicle and MPO-treated cells at 100x magnification. **f)** Results of invasion assay, normalized to the vehicle, upon treatment with 5  $\mu\text{g}/\text{ml}$  MPO (N = 5). One-way ANOVA and Tukey's post hoc test were performed. To compare two samples, an unpaired t-test was performed. Data are presented as the mean  $\pm$  SD, \*P < 0.05.

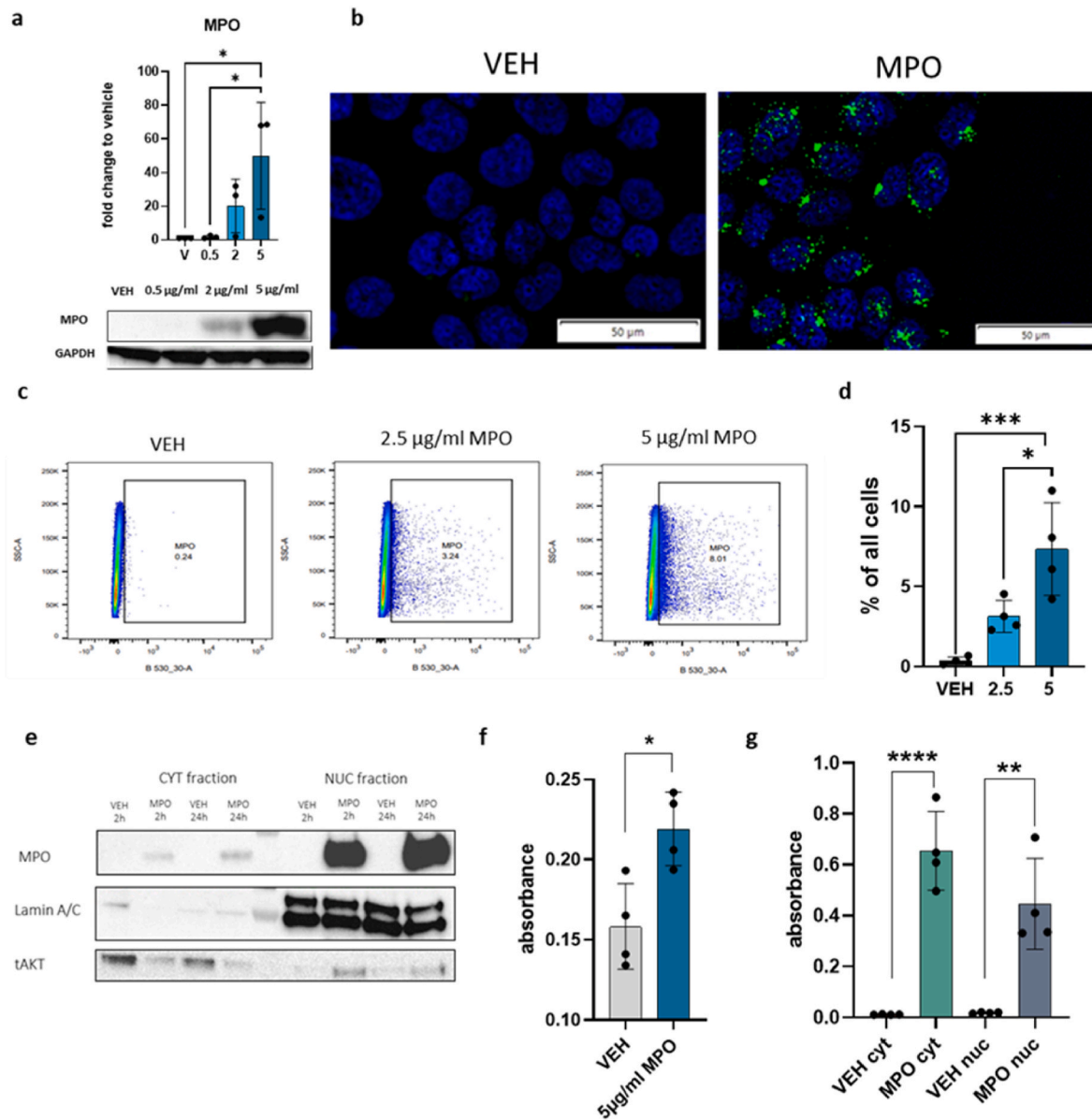


**Fig. 3.** MPO uptake by JEG-3 cells and nuclear localization

**a)** Western blot analysis of JEG-3 cells treated with various concentrations of MPO (vehicle, 0.5 µg/ml, 2 µg/ml and 5 µg/ml) and presented as fold-change relative to the vehicle (N = 3). **b)** Representative immunofluorescence microscopy images of vehicle and 10 µg/ml MPO-treated cells. The cell nucleus was stained with DAPI and MPO is represented in green with AF488-labeled secondary antibody. **c)** Scatterplots representing vehicle control, 2.5 µg/ml MPO, and 5 µg/ml MPO-treated JEG-3 cells. MPO-positive cells were gated based on the vehicle. Cells were treated for 4 h and intranuclear-stained for flow cytometry using an FITC-*anti*-MPO antibody was performed (N = 4). **d)** Results of flow cytometry analysis represented as % of all cells. **e)** Representative Western blot of JEG-3 cell fractions stained for MPO, Lamin A/C, and tAKT of vehicle and 5 µg/ml MPO-treated cells. Cytoplasmic and nuclear fractions were isolated. **f)** MPO activity assay of vehicle and MPO-treated JEG-3 cell lysates. Data are presented as absolute numbers (N = 4). **g)** MPO activity assay of nuclear and cytoplasmic fractions of 5 µg/ml MPO-treated JEG-3 cell lysates. In each experiment two biological replicates were analyzed and data are represented as absolute numbers (N = 4). One-way ANOVA and Tukey's post hoc test were performed for multiple comparisons. To compare two samples, an unpaired *t*-test was performed. Data are presented as the mean ± SD, \**P* < 0.05. (For interpretation of the references to colour in this figure legend, the reader is referred to the Web version of this article.)

internalization and uptake into the nucleus (Fig. 3g).

To determine whether this effect was observed in other invasive trophoblast cell lines, we performed similar experiments on the ACH-3P human trophoblast cell line [33]. Consistent with the JEG-3 results, an increase in total MPO in ACH-3P cells was observed by Western blot analysis (Supplementary Fig. 4a). Furthermore, immunofluorescence microscopy showed localization of MPO in the cytoplasm next to the nuclei (Supplementary Fig. 4b). Upon fractionation, we observed increased MPO localization in treated cells compared with the vehicle control. MPO was found in both cytoplasmic and nuclear fractions, and efficient fractionation was further confirmed by i) increased GAPDH

present in the cytoplasmic fraction, ii) Lamin A/C present in the nuclear fraction, and iii) increased tAKT present in the cytoplasmic fraction (Supplementary Fig. 4c).

#### 3.4. Myeloperoxidase uptake and activity is required for migration

MPO uptake by cells can be blocked by heparin, a member of the glycosaminoglycan (GAG) family [34]. Further, MPO activity can be impaired by aminobenzoic acid hydrazine (4-ABAH), a potent irreversible inhibitor of MPO [35]. Therefore, we determined the effect of these inhibitors on the internalization and function of MPO during

JEG-3 migration. We treated JEG-3 cells with MPO, heparin plus MPO, or 4-ABAH plus MPO. Immunofluorescence microscopy confirmed that heparin prevented MPO internalization into JEG-3 cells, whereas 4-ABAH did not block the internalization of MPO, as expected (Fig. 4a). To further determine the effect of heparin and 4-ABAH on MPO uptake, we performed flow cytometry analysis, measuring MPO levels in treated cells (Fig. 4b). Following addition of heparin, MPO uptake was completely abolished compared with cells treated with MPO alone. In contrast, MPO uptake was not affected by 4-ABAH in the JEG-3 cell line (Fig. 4b). To confirm these findings at the protein level, we performed Western blot analyses. Cells were treated with MPO alone as a positive control, MPO plus heparin (Fig. 4c), or MPO plus 25  $\mu$ M H<sub>2</sub>O<sub>2</sub> plus 4-ABAH (Fig. 4d). Additionally, we heat-inactivated MPO to destroy its enzymatic activity and three-dimensional structure to block GAG interactions as a negative control (Fig. 4d). MPO was not detected in

heparin-treated samples, where uptake was abolished, and in samples where MPO was denatured. Furthermore, 4-ABAH did not show decrease in MPO internalization (Fig. 4c-d).

Because we previously showed that MPO increases JEG-3 migration, we inhibited MPO uptake and activity using heparin and 4-ABAH. Most importantly, both heparin and 4-ABAH blocked MPO-induced cell migration (Fig. 4e). To confirm the function of 4-ABAH, we performed an activity assay and observed a complete inhibition of MPO activity upon treatment with 4-ABAH (Supplementary Fig. 5b).

#### 4. Discussion

Studies regarding neutrophils at the fetomaternal interface have indicated that proper neutrophil infiltration plays an important role in the normal development of the fetus. In recent mouse studies, neutrophil

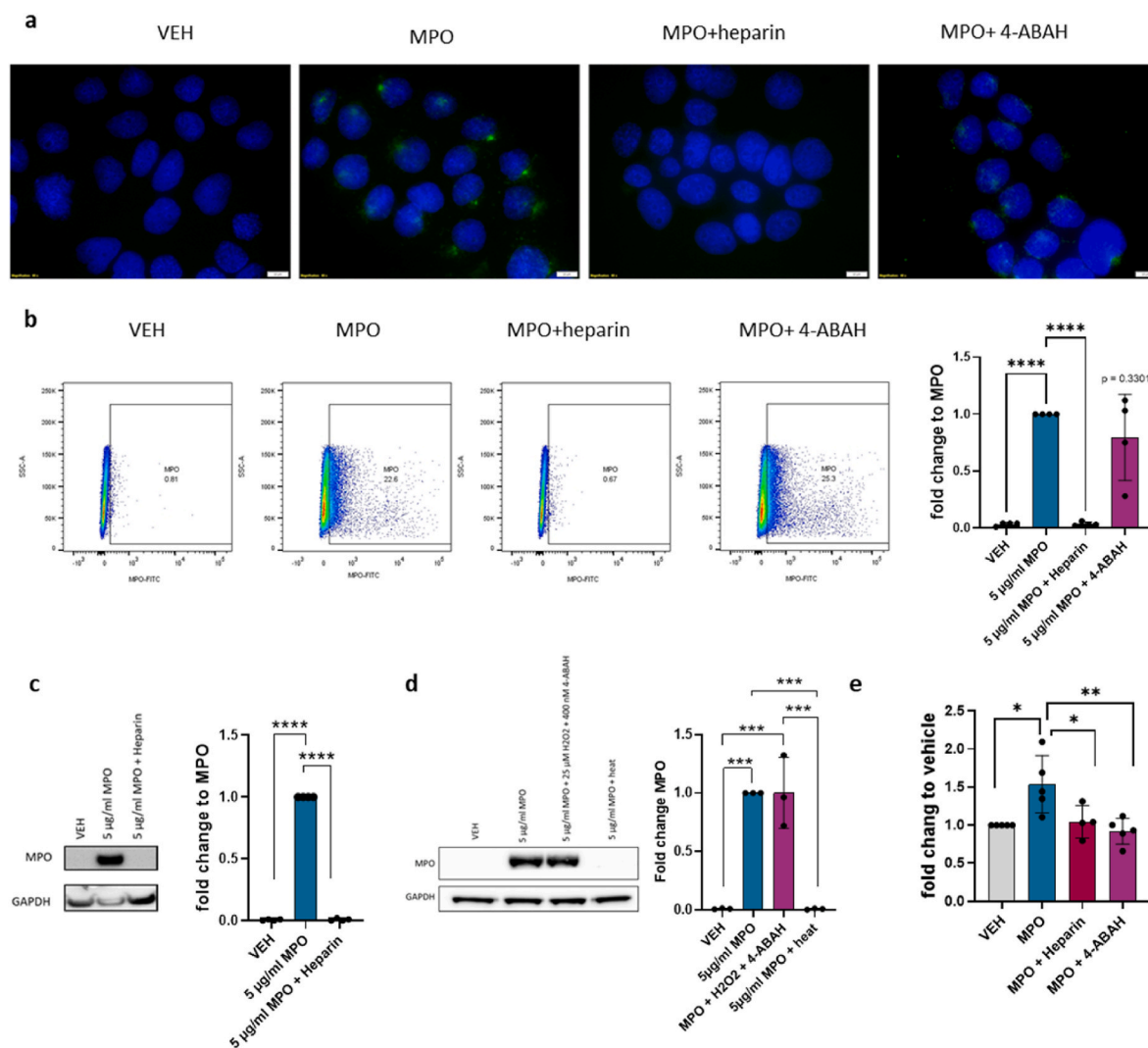


**Fig. 4.** MPO uptake and activity are important for enhanced migration

**a**) Representative immunofluorescence images of vehicle and 5  $\mu$ g/ml MPO-treated cells in combination with heparin (blocks MPO uptake) and the MPO activity inhibitor 4-ABAH. The cell nucleus was stained with DAPI and MPO is represented in green, labeled with AF488 secondary antibody. **b**) Scatterplots representing vehicle control and 5  $\mu$ g/ml MPO-treated JEG-3 cells in combination with heparin and 4-ABAH treatment. MPO-positive cells were gated based on vehicle-treated cells. Cells were treated for 4 h and intranuclear-stained for flow cytometry using a FITC-anti-MPO antibody (N = 4). Flow cytometry analysis of MPO-positive cells presented as fold-change relative to MPO-treated cells (N = 4). **c**) Representative Western blot images of MPO and GAPDH of JEG-3 cells treated with vehicle and 5  $\mu$ g/ml MPO in combination with heparin. Western blot analysis are presented as fold-change relative to MPO-treated cells (N = 4). **d**) Representative Western blot images of MPO and GAPDH of JEG-3 cells treated with vehicle and 5  $\mu$ g/ml MPO in combination with 4-ABAH + H<sub>2</sub>O<sub>2</sub>, or heat-inactivated MPO. Western blot analysis presented as fold-change relative to MPO-treated cells (N = 4). **e**) Results of ECIS measurements presented as mean (normalized to the % of wounding) fold-change relative to vehicle after 14 h (N = 5). One-way ANOVA and Tukey's test post hoc was performed for multiple comparisons. Data are presented as the mean  $\pm$  SD, \* $P < 0.05$ . (For interpretation of the references to colour in this figure legend, the reader is referred to the Web version of this article.)

depletion using anti-Gr1 or Ly6G antibodies resulted in inadequate blastocyst implantation as well as altered placenta development in pregnant mice [7,36], suggesting that neutrophils are important during the early stages of pregnancy [21]. Herein, we determined whether MPO, which is predominantly expressed by neutrophils and released into the extracellular space, plays a role during placentation. The JEG-3 choriocarcinoma cell line was used as a model to study EVT cell behavior in the presence of MPO, as primary trophoblasts lack efficient proliferation *in vitro*.

First, we showed that MPO is present and in proximity to EVTs in the DB. MPO expression in the DB during early and late gestation has previously been described [20,37]. Blood neutrophils from pregnant women accumulated higher amounts of MPO at the surface and released more superoxide than neutrophils from nonpregnant women [22]. In addition, we observed high levels of MPO in the supernatants of first-trimester tissue explants, confirming MPO release from tissue neutrophils into the microenvironment. In some cancers, MPO enhances tumor progression and metastases resulting in a higher migration of tumor cells [38]. In endothelial cells, MPO promotes tube formation and increases wound healing [19]. Similarly, we demonstrated that JEG-3 cells treated with MPO exhibited a higher migratory ability than that of vehicle-treated control cells. In addition, proliferation and apoptosis were not influenced by MPO, suggesting that the migratory effect is due to MPO activity and is not the direct result of proliferating cells. Similar to our data, MPO did not induce apoptosis in several endothelial cell lines; however, the same study found that MPO was internalized and present in the cytoplasm and nucleus of endothelial cells and that there were higher levels of intracellular oxidants [39]. We found that the total MPO within the cells was increased at higher concentrations of MPO. During inflammation, the levels of MPO are reportedly elevated [40]; however, to the best of our knowledge, there is no data regarding local MPO concentrations around neutrophils following degranulation. We hypothesized that upon neutrophil activation, there is a high concentration of MPO released in their surrounding environment. In addition to degranulation and release of MPO and other granular proteins into the extracellular space, neutrophils can undergo NETosis, leading to the accumulation of extracellular MPO bound to DNA [41]. Consistently, MPO was taken up by JEG-3 cells and localized in the cytoplasm and the nucleus as determined via immunofluorescence and cell fractionation studies. The same effect was observed in the ACH-3P EVT cell line. These data indicate that MPO uptake is not a cell-specific effect but rather a more general MPO effect. Further, we confirmed that MPO remains active upon internalization in both nuclear and cytoplasmic fractions. Conversely, previous reports regarding the effect of activated neutrophils on the Swan 71 trophoblast cell line showed a reduction in EVT migration. Herein, NET formation was induced, suggesting that MPO bound to DNA could not be internalized through glycosaminoglycan binding [42]. The neutrophil inflammatory and activation state may be a key event in understanding neutrophil–EVT interactions. Depending on their pro-inflammatory or anti-inflammatory phenotype, neutrophils can release different molecules, which depend upon microenvironmental stimuli [43]. During pregnancy, neutrophils promote Treg differentiation, favoring immune tolerance [44]. Furthermore, another study reported that when trophoblasts come in contact with activated neutrophils, neutrophil deactivation occurs *in vitro* [45]. This suggests a defense mechanism of EVTs toward activated neutrophils, causing them to adopt an immunosuppressive phenotype. To understand the *in vivo* interacting and complexity of neutrophil–EVT function, in depth spatiotemporal mapping in DB, needs to be performed in future studies.

Owing to its highly positive charge, MPO can bind to extracellular GAGs. In the endothelial glycocalyx, MPO binds to the side chains of heparan sulfate, removing syndecan-1 and disrupting glycocalyx formation [12]. Other GAGs were found to affect MPO internalization into cells. Reportedly, the coating of the cell-derived extracellular matrix with sodium heparin results in higher MPO binding. Furthermore, when incubating MPO with sodium heparin, MPO bound to heparin in solution

inhibited the binding of MPO to the extracellular matrix [46]. Based on these data, we selected sodium heparin as a blocker of MPO internalization and 4-ABAH as an irreversible inhibitor of MPO. We confirmed our hypothesis by demonstrating that the addition of heparin abolished MPO internalization into cells, whereas the addition of 4-ABAH did not affect internalization. Consistently, the total MPO levels were depleted to those of untreated cells, indicating that heparin competitively binds MPO and completely eradicates its binding and internalization into cells. These data suggest that binding to the cell surface and/or internalization of MPO is an important step in its actions. Finally, we revealed that heparin and 4-ABAH reduced MPO-mediated JEG-3 migration. An invasive phenotype of JEG-3 cell line has been previously described [47]. To determine if enhanced migration also affects invasion of JEG-3 cells, an invasion assay was performed. Consistent with the previous results, invasion was enhanced upon MPO treatment. When evaluating the efficiency of 4-ABAH inhibition of MPO activity, we confirmed MPO activity suppression, although the suppression was incomplete. Although 4-ABAH is a suicide inhibitor, it inhibits MPO only upon initial activation [48], and its clinical use might be limited. Other MPO inhibitors, such as verdiperstat and AZD5904, have been shown to be effective in mouse tumor models and should be used in future studies to evaluate the importance of MPO activity in trophoblast migration and invasion [49].

## 5. Conclusions

To the best of our knowledge, this is the first study to examine the effect of MPO on JEG-3 cell migration and invasion *in vitro*. We found altered JEG-3 migration following MPO stimulation and internalization of MPO into cells. MPO localizes to the cytoplasm and nuclei of both the tested cell lines, which were used as a model for EVT migration *in vitro*. The MPO effect was abolished using heparin and 4-ABAH. Overall, this study provides insight into the mechanisms underlying the role of neutrophil-derived proteins that may lead to successful pregnancy. Furthermore, it suggests neutrophils and neutrophil-derived proteins, including MPO, act as potent regulators of successful placentation. Therefore, MPO release, internalization, and function may represent potential therapeutic targets in pregnancy complications. Overall, this study provides insight into the mechanism underlying how extracellular MPO, predominantly derived from neutrophils, may alter EVT migration and invasion.

## Author contributions

ZN.M designed and performed the experiments, analyzed, and interpreted the results, crafted the figures, and wrote the manuscript. T. K. performed the experiments and analysis of the results. N.C.M. and P. V.-C. assisted with the experiments. O.K. performed the Bioinformatics evaluation of the data. M.G and J.P. provided tissue blocks and JEG-3 cells. J.K. designed, supervised, and wrote the manuscript. All authors critically reviewed the manuscript and approved the submitted version.

## Funding

This work was supported by the FWF doctoral programs: DK-MOLIN (W1241), DP-iDP (DOC-31), and RespImm (DOC-129) and OEAW (Doc Fellowship - 26477 to O.K.), who were trained within the frame of the PhD Program in Molecular Medicine at the Medical University of Graz. The work in the lab of J.K. was supported by the FWF [grant number P35294].

## Declaration of competing interest

None.



## Data availability

Data will be made available on request.

## Acknowledgements

We are grateful to Sabine Kern for her excellent technical assistance and to Marah Runtsch for proofreading the manuscript.

## Appendix A. Supplementary data

Supplementary data to this article can be found online at <https://doi.org/10.1016/j.redox.2023.102885>.

## References

- [1] Y. Sato, H. Fujiwara, I. Konishi, Mechanism of maternal vascular remodeling during human pregnancy, *Reprod. Med. Biol.* 11 (1) (2012 Jan) 27–36.
- [2] J.N. Bulmer, L. Morrison, M. Longfellow, A. Ritson, D. Pace, Granulated lymphocytes in human endometrium: histochemical and immunohistochemical studies, *Hum. Reprod.* 6 (6) (1991 Jul) 791–798.
- [3] J. Hanna, D. Goldman-Wohl, Y. Hamani, I. Avraham, C. Greenfield, S. Natanson-Yaron, et al., Decidual NK cells regulate key developmental processes at the human fetal-maternal interface, *Nat. Med.* 12 (9) (2006 Sep) 1065–1074.
- [4] S. Vondra, A.L. Höbler, A.I. Lackner, J. Raffetseder, Z.N. Mihalic, A. Vogel, et al., The human placenta shapes the phenotype of decidual macrophages, *Cell Rep.* 42 (1) (2023 Jan 10), 111977.
- [5] H. Amsalem, M. Kwan, A. Hazan, J. Zhang, R.L. Jones, W. Whittle, et al., Identification of a novel neutrophil population: proangiogenic granulocytes in second-trimester human decidua, *J Immunol Baltim Md* 193 (6) (2014 Sep 15) 3070–3079, 1950.
- [6] D. Croxatto, A. Micheletti, E. Montaldo, P. Orecchia, F. Loiacono, F. Canegallo, et al., Group 3 innate lymphoid cells regulate neutrophil migration and function in human decidua, *Mucosal Immunol.* 9 (6) (2016 Nov) 1372–1383.
- [7] S. Nadkarni, J. Smith, A.N. Sferruzzi-Perri, A. Ledwozyw, M. Kishore, R. Haas, et al., Neutrophils induce proangiogenic T cells with a regulatory phenotype in pregnancy, *Proc. Natl. Acad. Sci. U. S. A.* 113 (52) (2016 Dec 27) E8415–E8424.
- [8] P. Valadez-Cosmes, S. Raftopoulou, Z.N. Mihalic, G. Marsche, J. Kargl, Myeloperoxidase: growing importance in cancer pathogenesis and potential drug target, *Pharmacol. Ther.* 236 (2022 Aug), 108052.
- [9] K.D. Metzler, T.A. Fuchs, W.M. Nauseef, D. Reumaux, J. Roesler, I. Schulze, et al., Myeloperoxidase is required for neutrophil extracellular trap formation: implications for innate immunity, *Blood* 117 (3) (2011 Jan 20) 953–959.
- [10] J.K. Hurst, What really happens in the neutrophil phagosome? *Free Radic. Biol. Med.* 53 (3) (2012 Aug 1) 508–520.
- [11] C.L. Hawkins, M.J. Davies, Role of myeloperoxidase and oxidant formation in the extracellular environment in inflammation-induced tissue damage, *Free Radic. Biol. Med.* 172 (2021 Aug) 633–651.
- [12] K. Manchanda, H. Kolarova, C. Kerkenpaß, M. Mollenhauer, J. Vitecek, V. Rudolph, et al., MPO (Myeloperoxidase) reduces endothelial glycocalyx thickness dependent on its cationic charge, *Arterioscler. Thromb. Vasc. Biol.* 38 (8) (2018 Aug) 1859–1867.
- [13] D. Lau, H. Mollnau, J.P. Eiserich, B.A. Freeman, A. Daiber, U.M. Gehling, et al., Myeloperoxidase mediates neutrophil activation by association with CD11b/CD18 integrins, *Proc. Natl. Acad. Sci. U. S. A.* 102 (2) (2005 Jan 11) 431–436.
- [14] D. El Kebir, L. József, W. Pan, J.G. Filep, Myeloperoxidase delays neutrophil apoptosis through CD11b/CD18 integrins and prolongs inflammation, *Circ. Res.* 103 (4) (2008 Aug 15) 352–359.
- [15] H. Cai, C.Y. Chuang, C.L. Hawkins, M.J. Davies, Binding of myeloperoxidase to the extracellular matrix of smooth muscle cells and subsequent matrix modification, *Sci. Rep.* 10 (1) (2020 Jan 20) 666.
- [16] S.J. Donkel, F.J. Wolters, M.A. Ikram, M.P.M. De Maat, Circulating Myeloperoxidase (MPO)-DNA complexes as marker for Neutrophil Extracellular Traps (NETs) levels and the association with cardiovascular risk factors in the general population, *Garcia De Frutos P, PLoS One* 16 (8) (2021 Aug 11), e0253698.
- [17] A. Undurti, Y. Huang, J.A. Lupica, J.D. Smith, J.A. DiDonato, S.L. Hazen, Modification of high density lipoprotein by Myeloperoxidase generates a pro-inflammatory particle, *J. Biol. Chem.* 284 (45) (2009 Nov) 30825–30835.
- [18] K.D. Metzler, C. Goosmann, A. Lubojemska, A. Zychlinsky, V. Papayannopoulos, A Myeloperoxidase-containing complex regulates neutrophil elastase release and actin dynamics during NETosis, *Cell Rep.* 8 (3) (2014 Aug) 883–896.
- [19] A. Khalil, H. Medfai, P. Poelvoorde, M.F. Kazan, C. Delporte, P. Van Antwerpen, et al., Myeloperoxidase promotes tube formation, triggers ERK1/2 and Akt pathways and is expressed endogenously in endothelial cells, *Arch. Biochem. Biophys.* 654 (2018 Sep 15) 55–69.
- [20] A. Hammer, G. Desoye, G. Dohr, W. Sattler, E. Malle, Myeloperoxidase-dependent generation of hypochlorite-modified proteins in human placental tissues during normal pregnancy, *Lab Invest J Tech Methods Pathol* 81 (4) (2001 Apr) 543–554.
- [21] A.R. Moore, N. Vivanco Gonzalez, K.A. Plummer, O.R. Mitchell, H. Kaur, M. Rivera, et al., Gestationally dependent immune organization at the maternal-fetal interface, *Cell Rep.* 41 (7) (2022 Nov 15), 111651.
- [22] A.L. Kindzelskii, A.J. Clark, J. Espinoza, N. Maeda, Y. Aratani, R. Romero, et al., Myeloperoxidase accumulates at the neutrophil surface and enhances cell metabolism and oxidant release during pregnancy, *Eur. J. Immunol.* 36 (6) (2006 Jun) 1619–1628.
- [23] K. Rull, K. Tomberg, S. Köks, J. Männik, M. Möls, M. Sirotkina, et al., Increased placental expression and maternal serum levels of apoptosis-inducing TRAIL in recurrent miscarriage, *Placenta* 34 (2) (2013 Feb) 141–148.
- [24] H. Wickham, M. Averick, J. Bryan, W. Chang, L. McGowan, R. François, et al., Welcome to the tidyverse, *J. Open Source Softw.* 4 (43) (2019 Nov 21) 1686.
- [25] S. Davis, P.S. Meltzer, GEOquery: a bridge between the gene expression Omnibus (GEO) and BioConductor, *Bioinforma Oxf Engl* 23 (14) (2007 Jul 15) 1846–1847.
- [26] P. Luschniq, M. Kienzl, D. Roula, J. Pilic, R. Atallah, A. Heinemann, et al., The JAK1/2 inhibitor baricitinib suppresses eosinophil effector function and restricts allergen-induced airway eosinophilia, *Biochem. Pharmacol.* 192 (2021 Oct), 114690.
- [27] A. Tseng, K. Kim, J. Li, J. Cho, Myeloperoxidase negatively regulates neutrophil-endothelial cell interactions by impairing  $\alpha$ M $\beta$ 2 integrin function in sterile inflammation, *Front. Med.* 5 (2018 May 4) 134.
- [28] M. Bilban, S. Tauber, P. Haslinger, J. Pollheimer, L. Saleh, H. Pehamberger, et al., Trophoblast invasion: assessment of cellular models using gene expression signatures, *Placenta* 31 (11) (2010 Nov) 989–996.
- [29] J.Y. Park, S. Mani, G. Clair, H.M. Olson, V.L. Paurus, C.K. Ansong, et al., A microphysiological model of human trophoblast invasion during implantation, *Nat. Commun.* 13 (1) (2022 Mar 15) 1252.
- [30] A. Natenzon, P. McFadden, S.C. DaSilva-Arnold, S. Zamudio, N.P. Illsley, Diminished trophoblast differentiation in early onset preeclampsia, *Placenta* 120 (2022 Mar 24) 25–31.
- [31] I. Brosens, R. Pijnenborg, L. Vercruyse, R. Romero, The “Great Obstetrical Syndromes” are associated with disorders of deep placentation, *Am. J. Obstet. Gynecol.* 204 (3) (2011 Mar) 193–201.
- [32] A. Haegens, J.H.J. Vermooy, P. Heeringa, B.T. Mossman, E.F.M. Wouters, Myeloperoxidase modulates lung epithelial responses to pro-inflammatory agents, *Eur. Respir. J.* 31 (2) (2008 Feb 1) 252–260.
- [33] U. Hiden, C. Wadsack, N. Prutsch, M. Gauster, U. Weiss, H.G. Frank, et al., The first trimester human trophoblast cell line ACH-3P: a novel tool to study autocrine/paracrine regulatory loops of human trophoblast subpopulations-TNF-alpha stimulates MMP15 expression, *BMC Dev. Biol.* 7 (2007 Dec 19) 137.
- [34] H. Kolářová, J. Viteček, A. Černá, M. Černík, J. Příbyl, P. Skládal, et al., Myeloperoxidase mediated alteration of endothelial function is dependent on its cationic charge, *Free Radic. Biol. Med.* 162 (2021 Jan) 14–26.
- [35] A.J. Kettle, C.A. Gedge, C.C. Winterbourn, Mechanism of inactivation of myeloperoxidase by 4-aminobenzoic acid hydrazide, *Biochem. J.* 321 (Pt 2) (1997 Jan 15) 503–508. Pt 2.
- [36] C.B. Hebeda, A.C. Savioli, P. Scharf, M. de Paula-Silva, C.D. Gil, S.H.P. Farsky, et al., Neutrophil depletion in the pre-implantation phase impairs pregnancy index, placenta and fetus development, *Front. Immunol.* 13 (2022), 969336.
- [37] T.H. Hung, S.F. Chen, L.M. Lo, M.J. Li, Y.L. Yeh, T.T. Hsieh, Myeloperoxidase in the plasma and placenta of normal pregnant women and women with pregnancies complicated by preeclampsia and intrauterine growth restriction, *Placenta* 33 (4) (2012 Apr) 294–303.
- [38] V. Panagopoulos, D.A. Leach, I. Zinonos, V. Ponomarev, G. Licari, V. Liapis, et al., Inflammatory peroxidases promote breast cancer progression in mice via regulation of the tumour microenvironment, *Int. J. Oncol.* 50 (4) (2017 Apr) 1191–1200.
- [39] J.J. Yang, G.A. Preston, W.F. Pendergraft, M. Segelmark, P. Heeringa, S.L. Hogan, et al., Internalization of proteinase 3 is concomitant with endothelial cell apoptosis and internalization of myeloperoxidase with generation of intracellular oxidants, *Am. J. Pathol.* 158 (2) (2001 Feb) 581–592.
- [40] M. Weng, Y. Yue, D. Wu, C. Zhou, M. Guo, C. Sun, et al., Increased MPO in colorectal cancer is associated with high peripheral neutrophil counts and a poor prognosis: a TCGA with propensity score-Matched analysis, *Front. Oncol.* 12 (2022 Jul 14), 940706.
- [41] C.F. Urban, D. Ermert, M. Schmid, U. Abu-Abed, C. Goosmann, W. Nacken, et al., Neutrophil extracellular traps contain calprotectin, a cytosolic protein complex involved in host defense against *Candida albicans*, *PLoS Pathog.* 5 (10) (2009 Oct), e1000639.
- [42] G. Calo, F. Sabbione, N. Pascuali, I. Keitelman, D. Vota, D. Papparini, et al., Interplay between neutrophils and trophoblast cells conditions trophoblast function and triggers vascular transformation signals, *J. Cell. Physiol.* 235 (4) (2020 Apr) 3592–3603.
- [43] T. Keeley, D.L. Costanzo-Garvey, L.M. Cook, Unmasking the many faces of tumor-associated neutrophils and Macrophages: considerations for targeting innate immune cells in cancer, *Trends Cancer* 5 (12) (2019 Dec) 789–798.
- [44] X. Kang, X. Zhang, Z. Liu, H. Xu, T. Wang, L. He, et al., Granulocytic myeloid-derived suppressor cells maintain fetomaternal tolerance by inducing Foxp3 expression in CD4+CD25-T cells by activation of the TGF- $\beta$ / $\beta$ -catenin pathway, *Mol. Hum. Reprod.* 22 (7) (2016 Jul) 499–511.
- [45] H.R. Petty, A.L. Kindzelskii, J. Espinoza, R. Romero, Trophoblast contact deactivates human neutrophils, *J Immunol Baltim Md* 176 (5) (2006 Mar 1) 3205–3214, 1950.
- [46] L. Kubala, H. Kolářová, J. Viteček, S. Kremserová, A. Klinke, D. Lau, et al., The potentiation of myeloperoxidase activity by the glycosaminoglycan-dependent binding of myeloperoxidase to proteins of the extracellular matrix, *Biochim. Biophys. Acta* 1830 (10) (2013 Oct) 4524–4536.

- [47] S. Karmakar, R. Dhar, C. Das, Inhibition of cytotrophoblastic (JEG-3) cell invasion by interleukin 12 involves an interferon  $\gamma$ -mediated pathway, *J. Biol. Chem.* 279 (53) (2004 Dec) 55297–55307.
- [48] K.C. Agarwal, R.E. Parks, Adenosine analogs and human platelets. Effects on nucleotide pools and the aggregation phenomenon, *Biochem. Pharmacol.* 24 (24) (1975 Dec 15) 2239–2248.
- [49] T.W. Liu, S.T. Gammon, P. Yang, W. Ma, J. Wang, D. Piwnica-Worms, Inhibition of myeloperoxidase enhances immune checkpoint therapy for melanoma, *J Immunother Cancer* 11 (2) (2023 Feb), e005837.